journal

J. Am. Ceram. Soc., 78 [4] 986–92 (1995)

Reaction of TiO_2–Al–C in the Combustion Synthesis of TiC–Al_2O_3 Composite

Yoon Choi and Shi-Woo Rhee

Laboratory for Advanced Materials Processing, Department of Chemical Engineering, Pohang University of Science and Technology, Pohang 790-784, Korea

Reaction mechanisms and the thermal structure in the reaction zone during the combustion of TiO_2, Al, and C to form TiC–Al_2O_3 composite were studied. The reaction between each component was studied and the combustion wave structure and real-time temperature profile were analyzed. Titanium aluminide species, present in the aluminothermic reduction of TiO_2, did not occur in the presence of C, because of the high thermodynamic stability of TiC. The activation energies of the exothermic reaction in the $3TiO_2$–4Al–3C system were determined by DSC analysis. This suggests that the combustion reaction is mainly controlled by carbon diffusion through solid TiC. The combustion wave was observed to propagate in an unstable mode. The temperature profiles in the reaction zone were of the sawtooth type and the products were of layered structure.

I. Introduction

TiC–Al_2O_3 composites are used in applications such as cutting tools and tape heads in the electronic industry because of their high hardness (20–22 GPa), good strength (500–600 MPa), moderate fracture toughness (4–4.5 MPa·$m^{1/2}$), and fine grain size (1–5 μm). At the present time, commercial TiC–Al_2O_3 ceramics have been primarily manufactured by pressureless sintering or hot-pressing of TiC and Al_2O_3 powders whose composition is usually 30 wt% TiC–Al_2O_3.[1–3]

The metallothermic-reduction reaction,[4–7] which has been used in the preparation of various metals and alloys for several decades, is generally an exothermic process which is self-sustained by the heat liberated. The method which utilizes the self-sustained reactions to prepare refractory ceramic and intermetallic compounds is called self-propagating high-temperature synthesis (SHS), or combustion synthesis.[8] Recently, the synthesis of TiC–Al_2O_3 composites by combustion reaction has drawn much attention as an alternative to conventional processes because of its simplicity and energy efficiency.[9–11] The combustion synthesis of TiC–Al_2O_3 composite can be described as follows:[12]

$$3TiO_2(\text{rutile}) + 4Al + 3C \rightarrow 3TiC + 2Al_2O_3(\alpha)$$

$$\Delta H^\circ_{f,298.15\,K} = -1076.6\ \text{kJ/mol}$$

$$\Delta G^\circ_{f,298.15\,K} = -1038.9\ \text{kJ/mol}$$

The combustion reaction of metal oxide (TiO_2, SiO_2, B_2O_3, Fe_2O_3, etc.)–metal (Al, Mg, etc.)–carbon systems has been extensively studied using various methods. Among them aluminothermic reduction, i.e., reaction of metal oxide with aluminum, has been studied as a model to clarify a thermite reaction mechanism. Hida *et al.*[13,14] investigated the SiO_2–Al reaction interface to describe the reaction mechanism. Chernenko *et al.*[15] studied the effects of oxide properties on the ignition in aluminothermic reduction of various oxides, and Oriov *et al.*[16] performed thermodynamic analyses on the Nb_2O_5–Al–Ar and $LiNbO_3$–Al–Ar systems to calculate equilibrium composition as a function of temperature. The exothermic reaction in B_2O_3–Al–C and B_2O_3–Mg–C systems for Al_2O_3–B_4C and MgO–B_4C composites has been investigated by differential thermal analysis (DTA).[17] Culter *et al.*[18,19] and Logan *et al.*[20] analyzed the effects of reaction parameters and particle–particle interaction during the synthesis of oxide–carbide and oxide–boride composites.

So far, little effort has been undertaken to investigate the reaction kinetics and the real-time temperature profile in the TiO_2–Al–C combustion reaction. In the present work, thermal analyses and thermal explosion experiments on the TiO_2–Al and TiO_2–Al–C systems were performed to investigate the reaction mechanisms. The equilibrium composition of the TiO_2–Al–C–Ar reaction system was calculated as a function of temperature. The real-time temperature profiles were measured during the combustion reaction of TiO_2–Al–C to form TiC–Al_2O_3 composite. The microstructure and composition of the reaction products were investigated by optical microscope (OM), scanning electron microscope (SEM), X-ray diffraction (XRD), and wavelength dispersive spectroscopy (WDS).

II. Experimental Procedure

The precursors used in this work were powders of TiO_2 (99.9% pure, rutile, average particle size of 1 μm; Aldrich Products, Milwaukee, WI), Al (99.9% pure, average particle size of 20 μm; Kojundo Kagaku Products, Sakado), and graphite (99.9% pure, average particle size of 5 μm; Kojundo Kagaku Products). The homogeneous mixture with the desired composition was prepared by wet-milling the reactants in ethanol for 24 h using alumina milling media.

Cylindrical compacts, 20 mm in diameter and approximately 25 mm in height, were formed at pressures from 68 to 82 MPa in a stainless steel die with double-acting rams. The green densities of the compacts were maintained at 61 ± 3% of theoretical. Pellets were vacuum-dried for 24 h at 773 K and 10^{-4} torr. The dried pellets were placed in a stainless steel chamber with two quartz windows (100 mm in diameter). The chamber was 270 mm high with a diameter of 160 mm. Tungsten filaments were positioned approximately 2 mm above the top surface of the pellets for ignition. The chamber was purged and filled with argon gas to atmospheric pressure before the ignition. The top surface of the sample was ignited by applying a current of about 80 A to the filaments under about 50 V from a 7-kW transformer.

Two samples were placed end to end with a tungsten 5% Re–tungsten 26% Re thermocouple (0.254 mm) sandwiched between them to ensure that good contact was maintained between the thermocouple and the specimens during combustion. Boron nitride aerosol spray (Hermann C. Starck, Berlin, Germany) was used to protect the thermocouple bead. For each experiment, a new set of thermocouples was used to obtain

Z. Munir—contributing editor

Manuscript No. 194244. Received August 30, 1993; approved November 29, 1993.
Supported by the Research Institute of Industrial Science and Technology and by the Engineering Research Center for Interface Science and Technology of Materials.

confident temperature-profile data. The real-time voltage outputs from the W–Re thermocouple were measured using a data acquisition system and a personal computer. The reactions were also videotaped so that the combustion wave velocity could be measured. The videotape unit was capable of replaying the reaction by 1/30 s.

DTA for TiO_2–C, 4Al–3C, $3TiO_2$–4 Al, and $3TiO_2$–4Al–3C systems was performed by heating at a rate of 40°C·min^{-1} under an argon atmosphere. Differential scanning calorimetry (DSC) for the $3TiO_2$–4 Al–3C system was also performed by changing the heating rate from 5° to 40°C·min^{-1} under an argon atmosphere. The samples of $3TiO_2$–4Al and $3TiO_2$–4Al–3C were placed in a tubular furnace and heated over the temperature range 25° to 1200°C, at a heating rate of 8°C·min^{-1} under argon atmosphere.

The reaction couple of a TiO_2 disk and an Al disk was prepared to study the deoxidation process of TiO_2 during the reaction between TiO_2 and Al. For preparation of the TiO_2 disk, titanium oxide powder was uniaxially compacted under 90 MPa and sintered up to 1250°C under oxygen atmosphere, with a heating rate of 10°C/min, holding for 2 h, and a cooling rate of 20°C/min. The reaction couple experiment was performed under an argon atmosphere. The reaction couple was heated to 872°C at a heating rate of 15°C/min and, without holding, cooled down to room temperature at a cooling rate of 30°C/min.

The microstructure and chemical composition of reaction products were investigated using SEM, OM, XRD, and WDS.

III. Results and Discussion

(1) Reaction Mechanism

Figure 1 shows the DTA results for (A) TiO_2–C, (B) 4Al–3C, (C) $3TiO_2$–4Al, and (D) $3TiO_2$–4Al–3C at a heating rate of 40°C·min^{-1} under an argon atmosphere. The stoichiometric coefficient represents the molar ratio of each component. While no significant endothermic or exothermic peaks were observed in Fig. 1(A), one endothermic peak corresponding to Al melting was observed near 673°C in Fig. 1(B). Figures 1(C) and (D), however, show not only the endotherm of Al melting, but a strong exothermic peak with a maximum at 927°, 925°, and 997°C. The exotherm in Fig. 1(C) corresponds to aluminothermic reduction of TiO_2 and the exotherms in Fig. 1(D) correspond to a sequential reaction of the aluminothermic reduction and TiC synthesis.

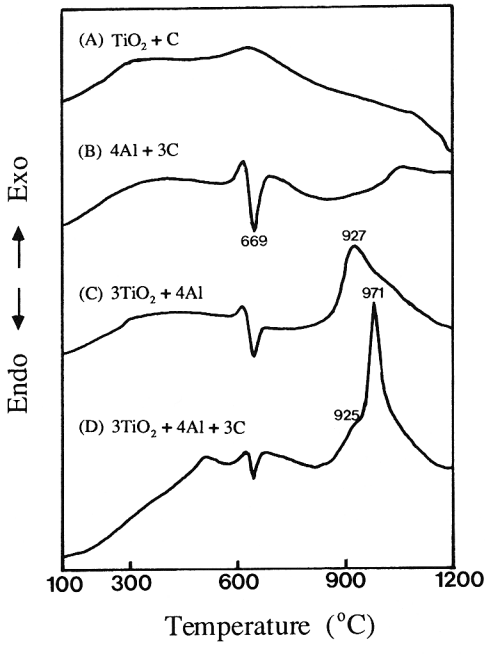

Fig. 1. DTA curves of compacted samples with a heating rate of 40°C/min under an argon atmosphere.

The aluminothermic reduction of TiO_2 occurred at a temperature approximately 210°C higher than the Al melting point (660.4°C). This may have been due to the wettability of Al melt on TiO_2. The wetting angle[21] of liquid Al–solid C and liquid Si–solid TiO_2 systems is reported to be approximately 157° and 107°, respectively. The surface energy[22] of liquid Si is similar to that of liquid Al at approximately 825 dyn·cm^{-1} under an argon atmosphere, and thus it is possible that the wetting angle between liquid Al and solid TiO_2 is near 107°. It is believed that the poor wettability of Al melt on TiO_2 should be one of the reasons why the aluminothermic reduction is initiated at temperatures higher than the Al melting point. In fact, large spherical Al was observed in the $3TiO_2$–4Al–3C sample heated above the Al melting point under the same conditions as the DTA experiment.

To analyze the consecutive reaction steps in the $3TiO_2$–4Al–3C system as well as the exothermic peaks in Figs. 1(C) and (D), we performed component analysis of the $3TiO_2$–4Al and the $3TiO_2$–4Al–3C samples which were quenched to atmosphere as soon as they were heated to a desired temperature. Table I shows the results of XRD analysis of the $3TiO_2$ + 4Al samples quenched after being heated to various temperatures at a heating rate of 8°C·min^{-1} under an argon atmosphere. It proves that the exotherm in Fig. 1(C) corresponds to aluminothermic reduction. It also indicates that the deoxidation reaction of TiO_2 by Al proceeds via Ti_3O_5, Ti_2O_3, and TiO to form Ti and Al_2O_3. Also part of the liquid Al reacts with reduced Ti to form titanium aluminides such as $TiAl_3$, Ti_2Al, and TiAl. It was reported by Logan *et al.*[20] that titanium aluminides were formed during the reaction between TiO_2 and Al. At 1200°C, the titanium aluminide phases such as $TiAl_3$ and Ti_2Al were transformed to form Ti and TiAl as secondary phases. At high temperatures, the amount of titanium aluminide phases becomes smaller because the reaction rate is faster and the reaction moves more toward thermodynamic equilibrium to give Ti and Al_2O_3.

The deoxidation process of TiO_2 by Al was confirmed by the reaction couple experiment of TiO_2 and Al. Figure 2 shows a polished cross section of the reaction couple prepared at 872°C. It is observed that while the concentration of Ti slightly increases as it approaches the interface, O slightly decreases. This confirms the deoxidation process of TiO_2 by Al.

Table II shows the XRD analysis of the $3TiO_2$–4Al–3C samples heated to various temperatures. The heating rate and atmosphere were the same as in the case of Table I. Comparison of the results of Table II and Fig. 1(C) suggests that the exothermic peaks in Fig. 1(D) correspond to a consecutive reaction of aluminothermic reduction of TiO_2 to form Al_2O_3 and TiC formation. Titanium aluminide phase was not observed at any temperature in this experiment. Also, when carbon black (99% pure, average particle size of 0.03 μm) was used as a carbon source, the titanium aluminides were not present. This suggests that if titanium aluminide phases are formed, they are only intermediate species during the TiC–Al_2O_3 combustion synthesis reaction because of the high thermodynamic stability of TiC. The chemical composition of the samples thermally exploded was almost the same as that of the samples combustion-synthesized from the $3TiO_2$–4Al–3C system.

Figure 3 shows the DSC curves for the $3TiO_2$–4Al–3C system which was heated at rates of (A) 40, (B) 30, (C) 20, (d) 10, and (E) 5°C·min^{-1} under an Ar atmosphere from room temperature to 1200°C. It also shows two successive exothermic peaks which correspond to aluminothermic reduction of TiO_2 and then TiC formation reaction, respectively. It indicates that in the exothermic reaction of $3TiO_2$–4Al–3C, the second exotherm caused mainly by TiC formation is conspicuous. When the heating rate was increased in the DSC experiment, each exothermic peak shifted to a higher temperature. This shift can be related to the apparent activation energy of the reaction using an analysis developed by Kissinger.[24] The shift is related to the heating rate as follows:

Table I. Results of X-ray Diffraction Pattern for the $3TiO_2$–4Al Samples Quenched after Being Heated to Various Temperatures

	Reaction products†									
Temperature (°C)	TiO_2	Al	Ti_3O_5	Ti_2O_3	TiO	Ti	$TiAl_3$	Ti_2Al	TiAl	Al_2O_3
646	M	M	S	-	-	-	-	-	-	-
700	M	M	S	-	-	-	-	-	-	-
786	M	M	S	m	-	-	-	-	-	m
866	M	M	S	S	m	-	-	-	-	m
933	S	S	S	S	S	m	-	-	-	M
1022	m	-	-	m	S	-	M	-	-	M
1095	-	-	-	m	S	-	-	S	m	M
1200	-	-	-	m	m	S	-	-	S	M

†M: major phase; S: secondary phase; m: minor phase.

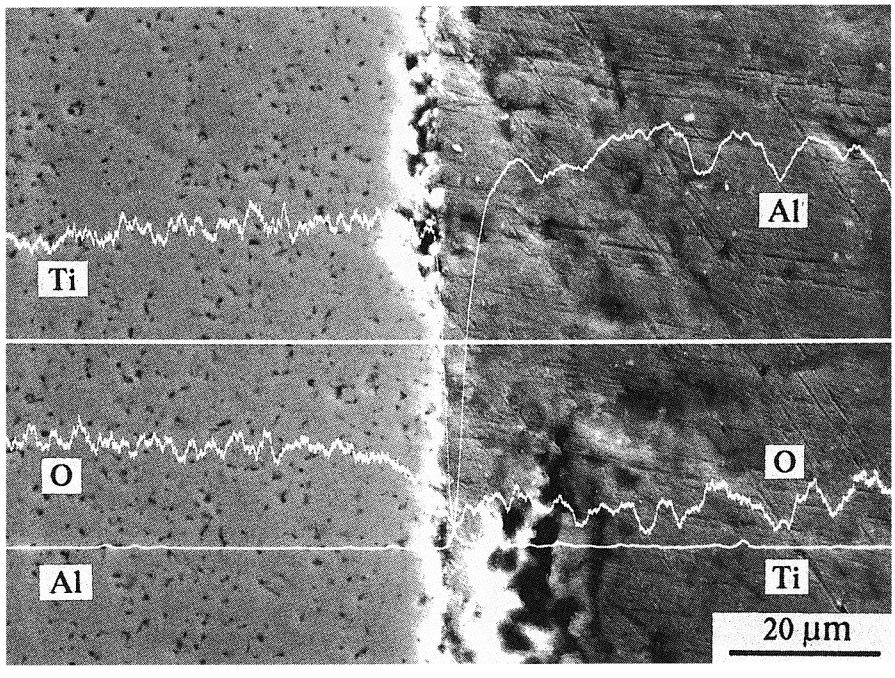

Fig. 2. Concentration profiles of Ti, O, and Al on the polished cross section of the reaction couple (titanium oxide disk–aluminum disk) formed at 872°C.

Table II. Results of X-ray Diffraction Pattern for $3TiO_2$–4Al–3C Samples Quenched after Being Heated to Various Temperatures

	Reaction products†											
Temperature (°C)	TiO_2	Al	C	Ti_3O_5	Ti_2O_3	TiO	Ti	$TiAl_3$	Ti_2Al	TiAl	Al_2O_3	TiC
645	M	M	M	S	-	-	-	-	-	-	-	-
678	M	M	M	S	-	-	-	-	-	-	-	-
807	M	M	M	S	m	-	-	-	-	-	-	-
893	M	M	M	m	S	m	-	-	-	-	S	-
1009	m	-	m	-	-	-	-	-	-	-	M	M
1074	-	-	-	-	-	-	-	-	-	-	M	M
1120	-	-	-	-	-	-	-	-	-	-	M	M
1200	-	-	-	-	-	-	-	-	-	-	M	M

†M: major phase; S: secondary phase; m: minor phase.

$$\ln (H/T_p^2) = C - E_a/RT_p$$

where H is the heating rate, T_p is the peak temperature, C is a constant, R is the gas constant, and E_a is the apparent activation energy.

Figure 4 shows the activation energy determined by Kissinger analysis from the peak temperature and heating rate data in Fig. 3. The activation energy calculated from the shift of the second exotherm was approximately 294 ± 31 kJ·mol^{-1}.

It is reported that the activation energy for titanium diffusion in solid TiC is approximately 738 kJ·mol^{-1} (Ref. 25) and those for carbon diffusion in solid TiC and liquid Ti are approximately in the range of 234–410 kJ·mol^{-1} (Refs. 26–29) and 78–117 kJ·mol^{-1} (Refs. 30 and 31), respectively, depending on the method of measurement. This indicates that the TiC–Al_2O_3 formation reaction from the $3TiO_2$–4Al–3C system is governed by TiC formation from reduced Ti and C, which is controlled by the diffusion of carbon through solid TiC. In the DSC analysis with carbon black (0.03 μm) as a carbon source, the activation energy calculated from the second exothermic peaks was 236 ± 22 kJ·mol^{-1}, which is about the same as with graphite as a carbon source. In the TiC combustion synthesis from Ti and C, carbon diffusion through solid TiC was suggested to be the rate-controlling step by Dunmead *et al.*[31]

Figure 5 shows the equilibrium composition of the product from the reaction of the $3TiO_2$–4Al–3C–Ar system as a function of temperature at a total pressure of 1 atm. Calculation was

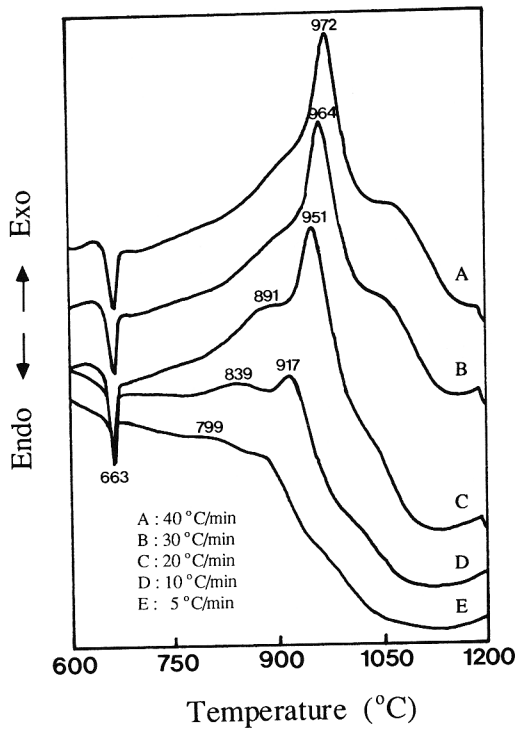

Fig. 3. DSC curves of compacted $3TiO_2$ + 4Al + 3S sample using graphite carbon source under an argon atmosphere.

done with the SOLGASMIX-PV code,[32] which gave the equilibrium composition of a multicomponent chemical system by direct minimization of the total free energy of the system. Equilibrium phase analysis can be well applied to a combustion reaction which has a very fast reaction rate and approaches equilibrium in a short time. The analysis shows that in the temperature range of 1500 to 3000 K, while the condensed phase mainly consists of TiC(*s*), α-Al_2O_3(*s*,*l*), the reaction products of the vapor phase consist of CO, Al_2O, and Al, and small amounts of TiO, Ti, Al_2, AlO, etc. This shows that vapor species such as CO, Al_2O, and Al participate in the reaction. However, it is clear that the combustion reaction of the $3TiO_2$–4Al–3C system is not dominated by the gaseous reaction because the amount of vapor species was approximately 2 orders of magnitude lower than that of solid phases, as shown in Fig. 5. The result of Fig. 5 also suggests that CO gas evolution during the reaction can bring about carbon loss.

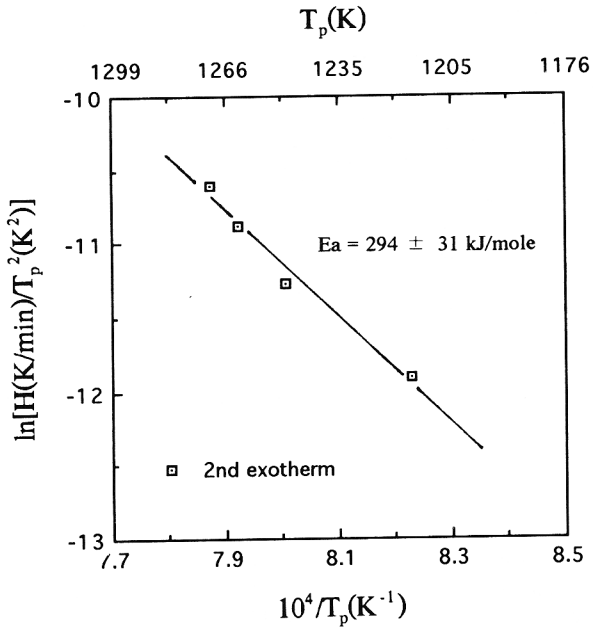

Fig. 4. Kissinger plot for the $3TiO_2$–4Al–3C system.

(2) Thermal Structure and Morphology

Figure 6 shows the real-time heating profiles during combustion reaction of the samples with the addition of (A) 0, (B), 12, (C) 18, and (d) 24 wt% Al_2O_3 in the $3TiO_2$–4Al–3C system. The temperature goes up very rapidly and several split peaks appear near the peak temperature. Heating rates and peak temperatures were over the range of approximately 1.3×10^3 to 2.7×10^4 K/s and approximately 2253 to 1892 K, respectively. On the other hand, the adiabatic temperature in the combustion reaction of $3TiO_2$ + 4Al + 3C, which is thermodynamically calculated from the heat of formation and the heat capacity, is about 2357 K. It is higher than the measured combustion temperature. This is mainly due to the convective and radiative heat losses during the reaction in a real system and gas evolution also should help the heat losses. The average wave velocities in the combustion synthesis with the addition of 0, 12, 18, and 24 wt% Al_2O_3 in the $3TiO_2$–4Al–3C sample were measured to be 0.39, 0.22, 0.13, and 0.07 cm/s, respectively.

Figure 7 shows the structure of the advancing wave in the combustion synthesis with the addition of (A) 0, (B) 12, (C) 18, and (D) 24 wt% in the $3TiO_2$–4Al–3C system, which is obtained by the videotaped images. The wave front in all of the cases proceeded in unstable combustion mode. With increased addition of the diluent, the advancing wave front became more unstable and was changed to local propagation with an oscillation.

Figure 8 shows scanning electron micrographs of polished cross-sectional surfaces of products combustion-synthesized with the same composition as in Fig. 6. In this case, the composition of the product is varied from 47 wt% TiC–Al_2O_3 to 35 wt% TiC–Al_2O_3. When 6 wt% of Al_2O_3 was added, the morphology was indistinguishably similar to the sample without Al_2O_3 addition. The morphology was periodically changed with cracks formed in a direction perpendicular to the wave front propagation. It is observed that the oscillation interval,

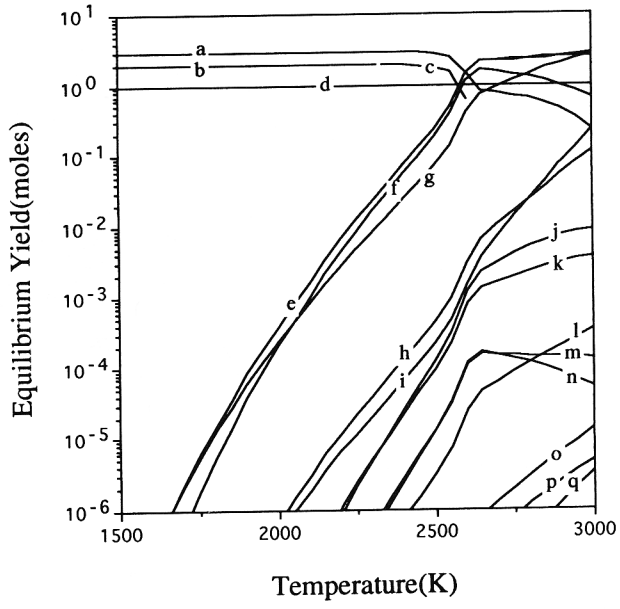

Fig. 5. Equilibrium product yield of $3TiO_2$–4Al–3C–Ar system as a function of temperature at a total pressure of 1 atm: (a) TiC(*s*), (b) α-Al_2O_3(*s*), (c) α-Al_2O_3(*l*), (d) Ar(*g*), (e) CO(*g*), (f) Al_2O(*g*), (g) Al(*g*), (h) TiO(*g*), (i) Ti(*g*), (j) Al_2(*g*), (k) AlO(*g*), (l) TiO_2(*g*), (m) CO_2(*g*), (n) Al_2O_2(*g*), (o) O(*g*), (p) AlC(*g*), (*q*) C(*g*).

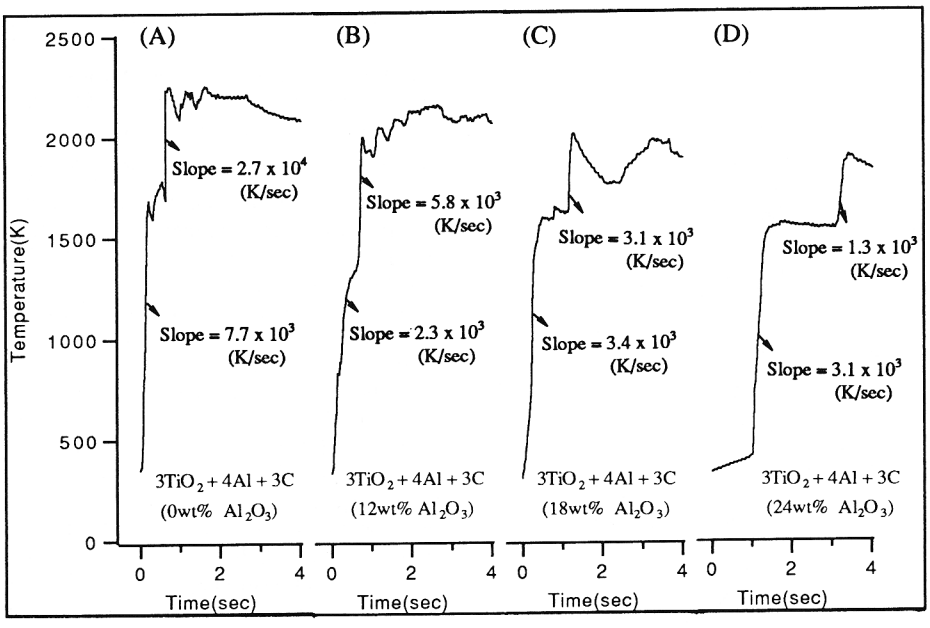

Fig. 6. Heating profiles in the reaction zone as a function of time.

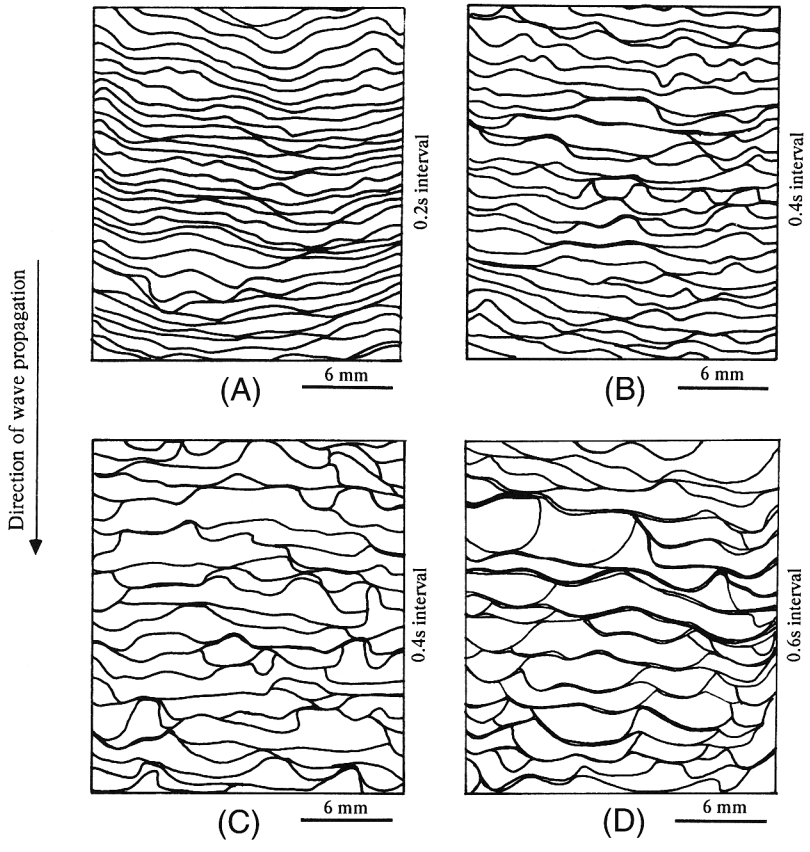

Fig. 7. Structure of the advancing combustion wave in the combustion synthesis with the addition of (A) 0, (B) 12, (C) 18, and (D) 24 wt% in the $3TiO_2 + 4Al + 3C$ sample.

which consisted of porous and dense regions, increases with increased Al_2O_3 addition. From the oscillatory peak intervals shown in Fig. 6 and the measured wave velocities, the oscillation intervals are calculated to be approximately 250, 370, 810, and 1750 μm, respectively, which are consistent with observations in Fig. 8. Therefore, the results of Figs. 7 and 8 support the idea that the thermal structures shown in Fig. 6 are affected predominantly by the combustion mode.

Combustion reaction of samples with excess Al addition to a stoichiometric mixture of $3TiO_2$–4Al–3C was performed to clarify the role of Al, which has a high affinity for oxygen. Figure 9 shows real-time temperature profiles during the com-

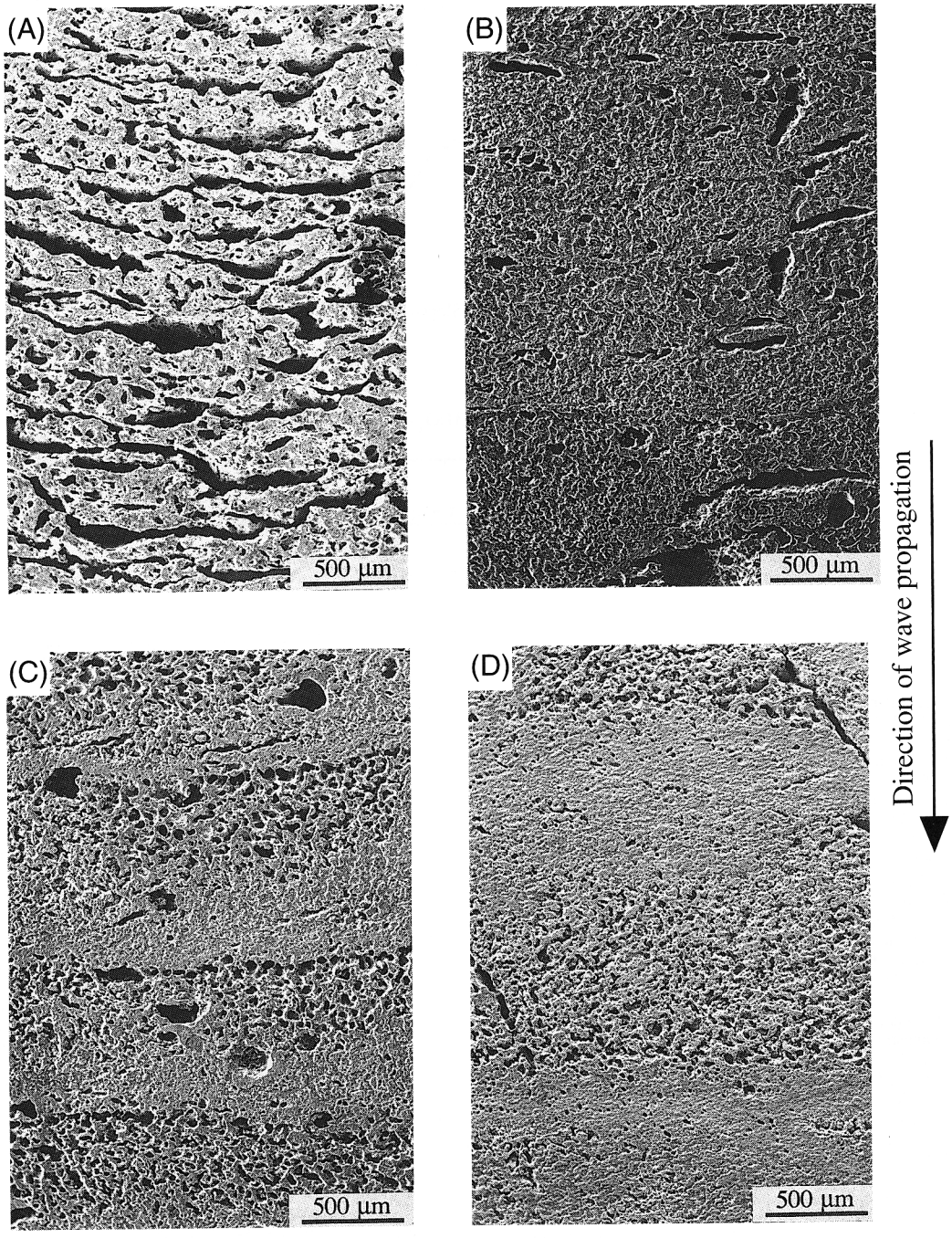

Fig. 8. Scanning electron micrographs of polished surface of products combustion-synthesized with the addition of (A) 0, (b) 12, (C) 18, (D) 24 wt% Al_2O_3 in $3TiO_2 + 4Al + 3C$ sample.

bustion reaction with the addition of (A) 3, (B) 4, and (C) 5 mol of Al to the $3TiO_2$–4Al–3C mixture. Compared to temperature profiles with Al_2O_3 dilution in Fig. 6, the heating rate is higher (approximately 1.7×10^4 to 2.5×10^4 K/s) and split peaks have higher amplitudes near peak temperature. This is because molten Al in the sample assists the reduction of TiO_2 and thus accelerates the initiation of the combustion reaction. The average combustion wave velocities in the samples were measured to be (A) 0.37, (B) 0.36, and (C) 0.34 cm/s, respectively. In spite of the addition of excess Al, the decrease in the wave velocity was not significant. Liquid Al not only plays a role as a reducing agent but also fills the pores in the sample and causes an increase of the sample thermal conductivity. The increase of thermal conductivity by pore-filling of liquid Al has already been reported by Grebe *et al.*[33]

IV. Summary

The interaction of TiO_2, Al, and C in the combustion synthesis of TiC–Al_2O_3 composites was investigated. Intermediate Ti or titanium aluminide species, present in the aluminothermic reduction of TiO_2 to form Al_2O_3, were not observed in the presence of C, because of the high thermodynamic stability of TiC. Based on a Kissinger plot, it is suggested that the composite formation reaction is controlled by carbon diffusion through solid TiC. The analysis of combustion wave structures confirmed that the wave front propagated in an unstable mode. The heating rates in the reaction zone were on the order of 10^3 to 10^4 K/s and the thermal structure was affected mainly by the combustion mode. It was also observed that the combustion products consisted of layered structures with a periodicity.

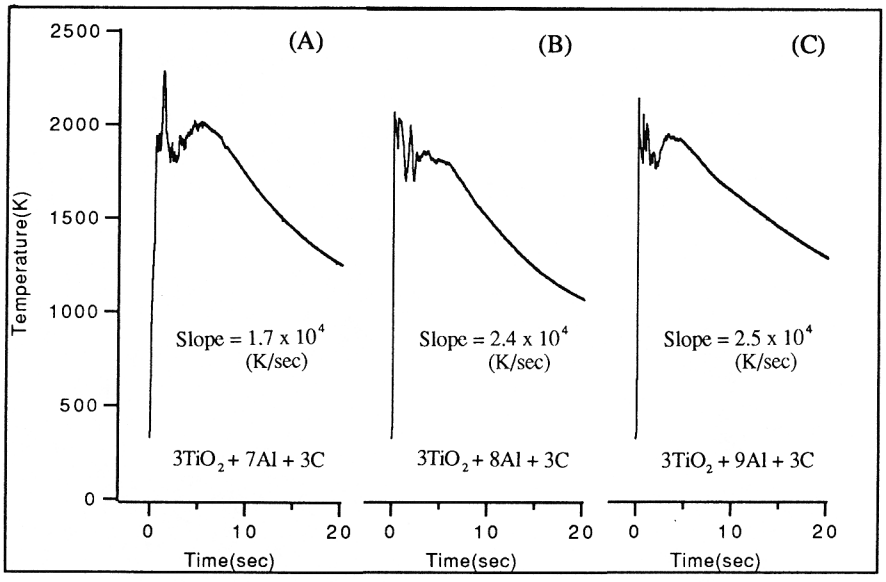

Fig. 9. Temperature profiles in the reaction zone as a function of time.

References

[1]A. G. King, "Ceramics for Cutting Metals," *Am. Ceram. Soc. Bull.*, **43** [5] 395–401 (1965).

[2]D. Bordui, "Hard-Part Machining with Ceramic Inserts," *Am. Ceram. Soc. Bull.*, **67** [6] 998–1001 (1988).

[3]S. J. Burden, "Comparison of Hot-Isostatically Pressed and Uniaxially Hot-Pressed Alumina–Titanium Carbide Cutting Tools," *Am. Ceram. Soc. Bull.*, **67** [6] 1003–1005 (1988).

[4]J. D. Walton, Jr., and N. E. Poulos, "Cermets from Thermite Reductions," *J. Am. Ceram. Soc.*, **42** [1] 40–49 (1959).

[5]O. N. Carlson, F. A. Schmidt, and W. E. Krupp, "A Process for Preparing High-Purity Vanadium," *J. Met.*, **18**, 320–23 (1966).

[6]F. H. Perfect, "Metallothermic Reduction of Oxides in Water-Cooled Copper Furnaces," *AIME Trans.*, **239**, 1282–86 (1967).

[7]F. A. Schmidt, R. M. Bergman, O. N. Carlson, and H. A. Wilhelm, "Molybdenum Metal by the Bomb Reduction of MoO_3," *J. Met.*, **28** [3] 38–44 (1971).

[8]W. L. Frankhouser, K. W. Brendley, M. C. Kieszek, and S. T. Sullivan, *Gasless Combustion Synthesis of Refractory Compounds*. Noyes Publications, Park Ridge, NJ, 1985.

[9]S. Adachi, T. Wada, T. Mihara, Y. Miyamoto, and M. Koizumi, "High-Presure Self-Combustion Sintering of Alumina–Titanium Carbide Ceramic Composite," *J. Am. Ceram. Soc.*, **73** [5] 1451–52 (1990).

[10]B. H. Rabin, G. E. Korth, and R. L. Williamson, "Fabrication of Titanium Carbide–Alumina Composites by Combustion Synthesis and Subsequent Dynamic Consolidation," *J. Am. Ceram. Soc.*, **73** [7] 2156–57 (1990).

[11]R. A. Cutler, K. M. Rigtrup, and A. V. Virkar, "Synthesis, Sintering, Microstructure, and Mechanical Properties of Ceramics Made by Exothermic Reactions," *J. Am. Ceram. Soc.*, **75** [1] 36–43 (1992).

[12]I. Barin, F. Sauert, E. Schultze-Rhonhof, and W. S. Sheng, *Thermochemical Data of Pure Substances*; pp. 48, 1528. VCH, New York, 1989.

[13]G. T. Hida and I. J. Lin, "Elementary Processes in SiO_2–Al Thermite-Type Reactions Activated or Induced by Mechanochemical Treatment"; pp. 246–61 in *Combustion and Plasma Synthesis of High-Temperature Materials*. Edited by Z. A. Munir and J. B. Holt. VCH Publishers, New York, 1990.

[14]G. T. Hida, I. J. Lin, and S. Nadiv, "Kinetics and Mechanism of the Reaction between Silicon Dioxide and Aluminum," *AiChE Symp. Ser.*, **84** [263] 69–72 (1988).

[15]E. V. Chernenko, L. F. Afanas'eva, V. A. Lebedeva, and V. I. Rozenband, "Inflammability of Mixtures of Metal Oxides with Aluminum," *Combust., Explos. Shock Waves (Engl. Transl.)*, **24** [6] 639–46 (1988).

[16]V. M. Orlov, V. I. Serba, and I. G. Kolesnikova, "Aluminothermic Reduction of Niobium Pentoxide and Lithium Niobate," *Izv. Akad. Nauk SSSR. Met. (Engl. Transl.)*, **5**, 30–33 (1985).

[17]L. L. Wang, Z. A. Munir, and J. B. Holt, "Combustion Synthesis of Oxide–Carbide Composites"; pp. 204–10 in *Combustion and Plasma Synthesis of High-Temperature Materials*. Edited by Z. A. Munir and J. B. Holt. VCH Publishers, New York, 1990.

[18]R. A. Cutler, A. V. Virkar, and J. B. Holt, "Synthesis and Densification of Oxide–Carbide Composites," *Ceram. Eng. Sci. Proc.*, **6** [7–8] 715–28 (1985).

[19]K. V. Logan and J. D. Walton, "TiB_2 Formation Using Thermite Ignition," *Ceram. Eng. Sci. Proc.*, **5** [7–8] 712–38 (1984).

[20]K. V. Logan, J. T. Sparrow, and W. J. S. McLemore, "Experimental Modeling of Particle–Particle Interactions during SHS of TiB_2–Al_2O_3"; pp. 219–28 in *Combustion and Plasma Synthesis of High-Temperature Materials*. Edited by Z. A. Munir and J. B. Holt. VCH Publishers, New York, 1990.

[21]L. C. Dufour, C. Monty, and G. P. Ervas, *Surfaces and Interfaces of Ceramic Materials*; p. 173. Kluwer Academic Publishers, Dordrecht, Netherlands, 1988.

[22]C. T. Lynch, *CRC Handbook of Materials Science*, Vol. I, *General Properties*; pp. 105, 109. CRC Press, Boca Raton, FL, 1974.

[23]I. Barin, F. Sauert, E. Schultze-Rhonhof, and W. S. Sheng, *Thermochemical Data of Pure Substances*; pp. 71–72. VCH, New York, 1989.

[24]H. E. Kissinger, "Reaction Kinetics in Differential Thermal Analysis," *Anal. Chem.*, **29** [11] 1702–706 (1957).

[25]S. Sarin, "Diffusion in ^{44}Ti in TiC_x," *J. Appl. Phys.*, **40** [9] 3515–20 (1969).

[26]S. Sarin, "Diffusion of Carbon in TiC," *J. Appl. Phys.*, **39** [7] 3305–10 (1968).

[27]S. Sarin, "Anomalous Diffusion of ^{14}C in $TiC_{0.67}$," *J. Appl. Phys.*, **39** [11] 5036–41 (1968).

[28]D. L. Kohlstedt, W. S. Williams, and J. B. Woodhouse, "Chemical Diffusion in Titanium Carbide Crystals," *J. Appl. Phys.*, **41**, 4476–84 (1970).

[29]C. J. Quinn and D. L. Kohlstedt, "Solid-State Reaction between Titanium Carbide and Titanium Metal," *J. Am. Ceram. Soc.*, **67**, 305–10 (1984).

[30]L. Adelsberg and L. Cadoff, "The Reactions of Liquid Titanium and Hafnium with Carbon," *Trans. AIME*, **24**, 933–35 (1967).

[31]S. D. Dunmead, D. W. Readey, C. E. Semler, and J. B. Holt, "Kinetics of Combustion Synthesis in the Ti–C and Ti–C–Ni Systems," *J. Am. Ceram. Soc.*, **72** [12] 2318–24 (1989).

[32]B. W. Sheldon, "SOLGASMIX-PV for the PC," Oak Ridge National Laboratory, Oak Ridge, TN, 1989.

[33]H. A. Grebe, A. Advani, N. N. Thadhani, and T. Kottke, "Combustion Synthesis and Subsequent Explosive Densification of Titanium Carbide Ceramics," *Metall. Trans. A*, **23A**, 2365–72 (1992). □